

AD

Reports Control Symbol
OSD-1366



AD658667

Research and Development Technical Report

ECOM-2852

AUTOMATIC COUNTING OF ATMOSPHERIC AEROSOLS
COLLECTED WITH THE GOETZ ULTRACENTRIFUGE

by

HERMANN E. GERBER

JUNE 1967

ECOM

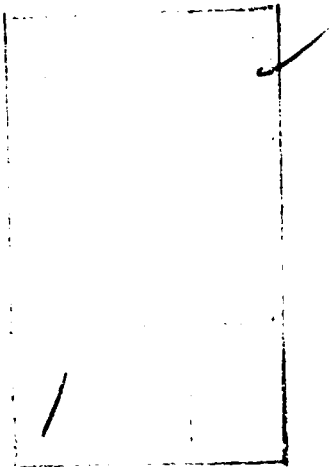
UNITED STATES ARMY ELECTRONICS COMMAND • FORT MONMOUTH, N.J.

DISTRIBUTION OF THIS DOCUMENT IS UNLIMITED

Best Available Copy

CELESTINE HOUSE
1000 1/2 N. 10th St.
Ft. Monmouth, N.J. 08034

34



NOTICES

Disclaimers

The findings in this report are not to be construed as an official Department of the Army position, unless so designated by other authorized documents.

The citation of trade names and names of manufacturers in this report is not to be construed as official Government indorsement or approval of commercial products or services referenced herein.

Disposition

Destroy this report when it is no longer needed. Do not return it to the originator.

Technical Report ECOM-2852

**AUTOMATIC COUNTING OF ATMOSPHERIC AEROSOLS
COLLECTED WITH THE GOETZ ULTRACENTRIFUGE**

by

Hermann E. Gerber

Atmospheric Physics Division

Atmospheric Sciences Laboratory

June 1967

DA Task No. 1V0-14501-B-53A-03

U. S. ARMY ELECTRONICS COMMAND

FORT MONMOUTH, NEW JERSEY

Distribution of this document is unlimited

Abstract

An automatic counter was developed with which submicron aerosol data, collected with the Goetz Aerosol Spectrometer ultracentrifuge, was rapidly and accurately evaluated.

The data, consisting of 35 mm microphotographs of large numbers of aerosols, were reduced by utilizing a unique track-scanning geometry in conjunction with a mechanical planar scanner. The photographic images of the aerosols and their locations on the data field were considered in detail, and appropriate corrections were derived to compensate for coincidence counting losses and the variable opacity of the images.

Using the automatic counter, it was possible to count up to 500 aerosol images on a 2.0 cm^2 area on each microphotograph. The counts were accomplished with a standard deviation of approximately 0.20 times the magnitude of the inherent statistical uncertainty of the data. Also, each microphotograph was automatically scanned and counted in 140 seconds.

CONTENTS		<u>Page No.</u>
Abstract		ii
INTRODUCTION		1
DISCUSSION		4
The Scanning Geometry		4
Scanning Geometry for the GAS Data		6
Accuracy of the Track-Scanning Method		9
Description of Instrumentation		22
Evaluation of the Automatic Counter		27
REFERENCES		32

Figures

1. Dark field microphotograph (negative) of aerosols collected with the Goetz ultracentrifuge	2
2. Track-scanning geometry of Cooke-Yarborough, et al (1954)	7
3. Track-scanning geometry used in counting the GAS aerosol data	8
4. Nomograms relating machine counts to actual number of particles on data areas	13-16
5. Sketch of the opacity cross-section of two particles coinciding because of the addition of opacities in the tails of the particles	17
6. Diagram used in the computation of the ϵ error	18
7. Automatic particle counter	24
8. Principal components of the automatic counter	25
9. Machine counts of three frames of GAS data film	28
10. Repetitive machine count of one frame of GAS film data	29
11. GAS field test, 30 July 1965, Flagstaff, Arizona	30

AUTOMATIC COUNTING OF ATMOSPHERIC AEROSOLS COLLECTED WITH THE GOETZ ULTRACENTRIFUGE

INTRODUCTION

Important constituents of the atmosphere are small liquid and solid particles called aerosols. Their number, size, and composition have direct bearing in many areas of atmospheric physics, such as cloud physics, cloud modification, air pollution, air chemistry, and others.

An instrument that is capable of measuring both the number and size distribution of aerosols ranging in size from 0.03 to 3 microns in diameter is the Goetz Aerosol Spectrometer (GAS) ultracentrifuge (Goetz, et al, 1960a, and Goetz, et al, 1960b).

The Goetz instrument subjects a small volume of air to thousands of "G's" of force, which causes the aerosols contained therein to settle out against a chrome-plated collecting foil. The geometry and force gradient in the instrument's chamber are such that the aerosols are deposited in an orderly pattern corresponding to their equivalent Stokes diameters. (For a spherical particle, the equivalent Stokes diameter equals its geometric diameter; while for an aspherical particle it equals the diameter of a spherical particle that exhibits the same Stokes-law-determined settling rate in the air.) By analyzing the density distribution of the deposited particles on the GAS foil, it is possible to deduce the number and Stokes diameter size distribution in the volume of air sampled. This is accomplished by counting the number of particle images appearing in each of a series of microphotographs of different areas of the foil. An example of such a photograph is shown in Fig. 1, in which several hundred different particle images can be seen.

To insure an adequate statistical readout accuracy of the number and size distribution of the aerosols, up to 500 particles must exist and be counted on each microphotograph. Since a typical GAS field measurement consists of a set of 100 such microphotographs, a visual readout tends to be excessively time-consuming. The practical usefulness of the GAS instrument would therefore be greatly enhanced by using an automatic method of counting the particle images.

Many different automatic particle-counting techniques have been developed for evaluating planar deposits of various types of particles. Almost all the devices constructed to date have attempted to emulate the actions of the eye by scanning the sample area with a photosensor and detecting the light intensity changes caused by the particles passing through their field of view. These devices are labelled "planar scanners," and for a



Fig. 1. Dark field microphotograph (negative) of aerosols collected with the Goetz ultracentrifuge

comprehensive history of various types, the following authors are referenced: P. Connor (1963), J. Pearson (1957), and W. Walton (1954).

Planar scanners, of course, have the advantage of evaluating particle data faster than is possible by visual means; however, they have had difficulty in approaching the accuracy capabilities of the eye. For instance, if the particles are randomly distributed over the collecting surface, as is the case in the GAS, there is a possibility that two particles could be in close proximity to each other. The eye could easily distinguish the existence of the two particles, but the machine with a finite field of view and a rigid traverse of the data area might see the two particles as only one. Such a loss of particle count is called "coincidence," and can be of significant extent. However, the effect of systematic errors such as the coincidence loss can usually be computed for and largely corrected. The predictable error is thus another advantage of using automatic methods, since the eye can result in errors that are totally unpredictable. Fatigue, boredom, and change in observing personnel have been known to cause serious errors in lengthy particle evaluations (R. Biggs, et al, 1948).

Choosing a planar scanner for the GAS evaluation presented some difficulty, since the particle images on the film data differ from any of the data formats utilized in the machines discussed by the above-referenced authors. Whereas the particle images usually present a constant opacity or brightness over their entire area and a sharp discontinuity between themselves and the surrounding data plane, the GAS data images exhibit variable opacity and a gradual opacity drop-off at their edges. More specifically, the GAS data format is as follows: On the film record, which involves particles in the 0.1 to 1.5 μ diameter range, the background is transparent, while the location of a particle image appears as a small circular dark region. Assuming a background transmittance of 100 percent, the light transmission through the particle images ranges from 3 to 62 percent. The center of each image is darkest and for all size particles is approximately 150 μ in diameter.

Images of the larger particles show concentric rings around the central dark area, each with as many as five rings, adding 100 μ to the diameter of the images. These images are similar in appearance to an Airy diffraction image of a circular aperture (M. Born and E. Wolf, 1964). However, on our images the rings are diffuse and tend to merge with each other and the central region, while in the Airy diffraction pattern a sharp contrast exists between image elements. A lack of a two-dimensional image and of Koehler and monochromatic illumination causes the difference. The cross section of the opacity of a typical GAS particle image, therefore, approximates a Gaussian curve with slight fluctuations caused by the rings around the central dark area.

This report describes the design, construction, and testing of a suitable automatic planar scanner developed for counting the aerosol images of the Goetz Aerosol Spectrometer (GAS).

DISCUSSION

Scanning Geometry

The first and most important consideration in designing the automatic planar scanner is choosing a suitable scanning geometry with which a photo-sensitive device, such as a phototube, views the particle data area. In some automatic planar scanning systems, the whole data area is illuminated and it is necessary to limit the field of view of the scanning phototube to a small section of that area; while in other systems the phototube measures the light transmitted through the data area by a scanning beam of light. In either case, the geometry of the light beam or of the field of view of the phototube must be chosen so as to produce the desired measurement of the data area. For almost all planar scanners, the scanning geometry can be categorized into three types: single spot, double and pseudo-double spot, and slit (P. Connor, 1963, W. Walton, 1954). To answer the question as to which of the three geometries is best for the data collected by the GAS, it would be helpful to study the literature on the various planar scanners that have been built.

1. Scanning by Single Spot. In the simplest of planar scanning methods, the single-spot geometry is used to obtain counting pulses from each of the particles that are intercepted by the scan over the data area. An instrument built by L. Flory and W. Pike in 1953 used this principle to count circular blood cells on a microscope slide. To avoid excessive coincidence losses, they used a scanning spot of light which was similar in size to the blood cells. The small size of the spot and the closeness of succeeding scans across the data area caused each blood cell to give more than one count. Since the average size of the blood cells was known, it was possible to compensate for the additional counts caused by this overlap of the cells into adjacent traverses of the scan.

Under other circumstances, when the average size of the particles in the data area is not known, a correct count is not possible since we do not know how many additional counts of the particles are caused by overlap. A possible variation would be to place the adjacent scans far enough apart to avoid overlap. However, this would not be satisfactory either, since the effective diameter of the spot would become an unknown variable and no correct measurement could be made of the particles per unit data area. Since the particle images in our data do have size variation, these single-spot counting methods could not be used.

Another method of scanning with a single spot with which it is possible to count circular particles of different sizes has received much attention.

Most of the instruments using this method were built with the purpose of analyzing planar deposits of droplets (C. Adler, et al, 1954; W. Wheeler, et al, 1953; and R. Courshee, 1954). The method all these instruments use is called "cord intercept scanning." The single spot is chosen which is much smaller than the particles on the data area, and closely adjacent scans are used. Besides counting the number of intercepts, the duration of each is recorded. In the instrument of R. Courshee, as many as 15 electronic channels were used to sort the length of the intercepts. With the number of intercepts in each of the 15 size-groups known, it was possible to statistically deduce the size distribution of the particles and from this the total number.

The cord intercept method could be applied to our data; however, the complexity of using multiple electronic channels to size the particles when only a count is necessary is not desirable. Also, according to C. Adler et al (1954), a minimum of 500 or 600 particles is necessary to produce accurate counting results. Our data range up to 500 particles in some data areas, but many areas have less.

2. Scanning by Double and Pseudo Double Spot. The second type of scanning geometry has two variations--double spot and pseudo double spot--and can count independently of the particle size. The double-spot method--sometimes called guard-spot method--counts the field of particles by scanning the data area with two adjacent spots, each of which uses a phototube and associated circuitry. A count is obtained from each particle only when one of the spots passes over. When both spots see the particle, a canceling pulse is produced and no count is recorded, thus avoiding the additional counts caused by overlap. Instruments have been constructed using the guard-spot technique and are described by P. Connor (1963). However, some authors (H. Dell, et al, 1960) have felt that a serious weakness of this method was the need for entirely separate electronic systems for the pair of spots. They stated that since the count for each particle came from the first interception of that particle and was therefore close to the resolution limit of the instrument, even a small variation in sensitivity of the electronic channels or of the scan path could cause large counting errors.

The weakness of the employment of two identical electronic systems is avoided by using the pseudo double-spot scanning geometry first described by H. Dell, et al (1951). Here the role of the guard spot was taken over by a memory system that recorded only the initial pulse of each intercepted particle. As the scan that followed the initial interception again approached the vicinity of the particle, the memory system would produce a canceling pulse so that the overlapping particle was not counted again. Instruments using the pseudo double-spot scanning geometry may be obtained commercially from Casella, Ltd., Cinema-Television, Ltd., and Mullard, Ltd.

A condition for the operation of the double and pseudo-double spot methods is the existence of an association criterion between the initial counting pulse and the canceling pulse (D. Gillings, 1950). The criterion is the necessity of producing the canceling pulse a certain distance before the same location is reached where the initial pulse occurred in the preceding scan. In this manner, the overlapping part of a particle that might be larger than was seen in the previous scan will not give any additional counts.

The error of coincidence will be canceled by such a criterion, since the particles become effectively larger on the data area. This effect can be especially prevalent for particles that have a wide range in the size distribution and also for data areas that have a high density of particles (J. Phillips, 1954). Since our data can have both of the above-stated characteristics, it would be desirable to avoid the necessity of the association criterion.

3. Scanning by Slit. When scanning the data area with a slit, circular particles can be counted independently of their size; and also an association criterion is not necessary. The theory of scanning with a slit, also called "track scanning," was developed by P. Hawksly (1954a) and utilized in counters built by E. Cooke-Yarborough et al (1954), L. LeBouffant et al (1954), P. Hawksly (1954b), and H. Morgan et al (1959). Basically, the data area is scanned with a slit of one dimension and then scanned again with a longer slit of the same width. With this method, only one electronic channel is needed and with a proper combination of the counts obtained from the two different slits, the number of particles and their average size on the data area are known. The disadvantage of track scanning is the necessity of relating the scan paths of the different slits. If the two slits do not scan the same paths over the data area, counting accuracy is lost (P. Hawksley, 1954a).

Scanning Geometry for the GAS Data

It was felt that the difficulty of scanning the two slits could be overcome and, since track scanning had the desirable characteristics mentioned, it was chosen for the GAS data. The method chosen was similar to the one proposed by E. Cooke-Yarborough et al (1954) to count blood cells on a microscope slide. In their method, a scan of the data area is first made with a slit of width W as shown in Fig. 2, while the second scan is made with slits of width $W/2$. By subtracting the counts received from the $W/2$ slits from the W slit, the number of cells lying in the shaded area are counted. Since counting accuracy also depends on the data sample size, the shaded area should be adjusted to cover as much of the data area as possible. For particles of one known size, as for the blood cells, this can be done; however, for data that have size variability such as ours, a

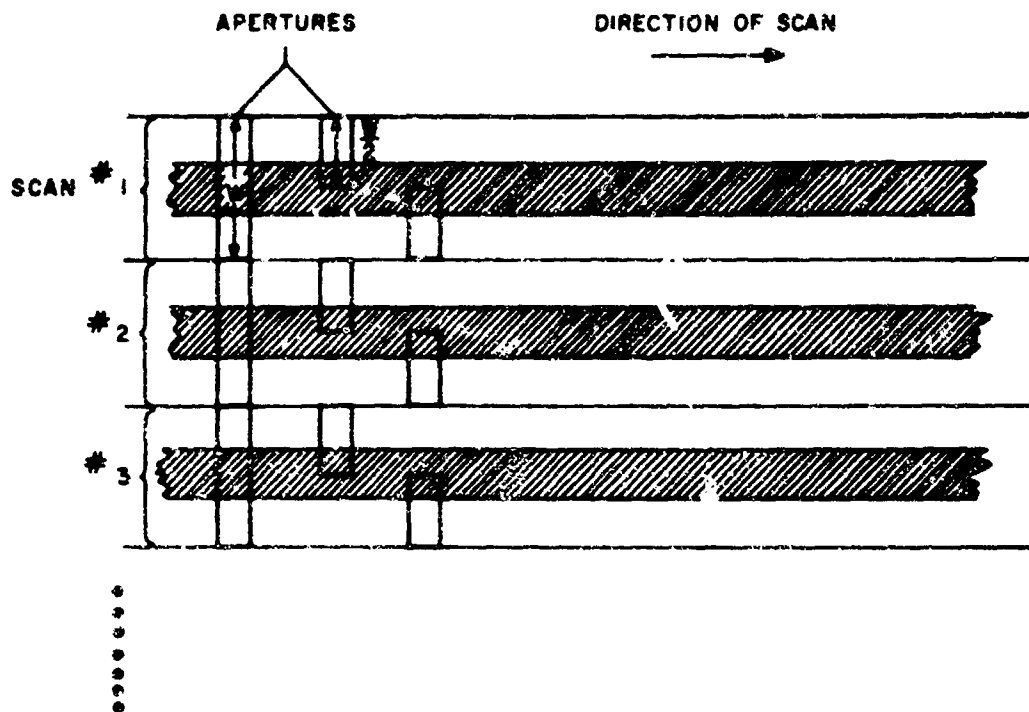


Fig. 2. Track-scanning geometry of Cooke-Yarborough, et. al. (1954). Particles located in the shaded area are counted.

constant adjustment of the data area to be analyzed (the shaded area) is necessary, but undesirable.

A unique variation of the above-described track-scanning geometry is used in our planar scanner, and is shown in Fig. 3. A slit of length W_1 is first scanned across the data area so that the successive scans are adjacent to each other as shown. The number of particles and fractions of particles that are intercepted by W_1 is recorded. Next the data area is scanned by a larger slit of length W_2 , which overlaps on each successive scan in the manner shown. Again the particles that are intercepted are counted. The whole data area is scanned in this manner, and by subtracting the counts obtained with W_1 from W_2 , the number of particles is known independently of their size and location on the data area. This feature can be demonstrated by noting the number of counts produced by particles P_1 , P_2 in Fig. 3.

It is shown that the smaller particle is intercepted twice by W_1 and three times by W_2 ; the difference in counts is one. Similarly for P_2 , four counts produced by W_1 subtracted from five counts from W_2 results in one. Equations (1) through (5) also describe this procedure. N is the desired number of particles in the data area $\propto L W_1$, where

$$\alpha = \text{number of adjacent scans,}$$

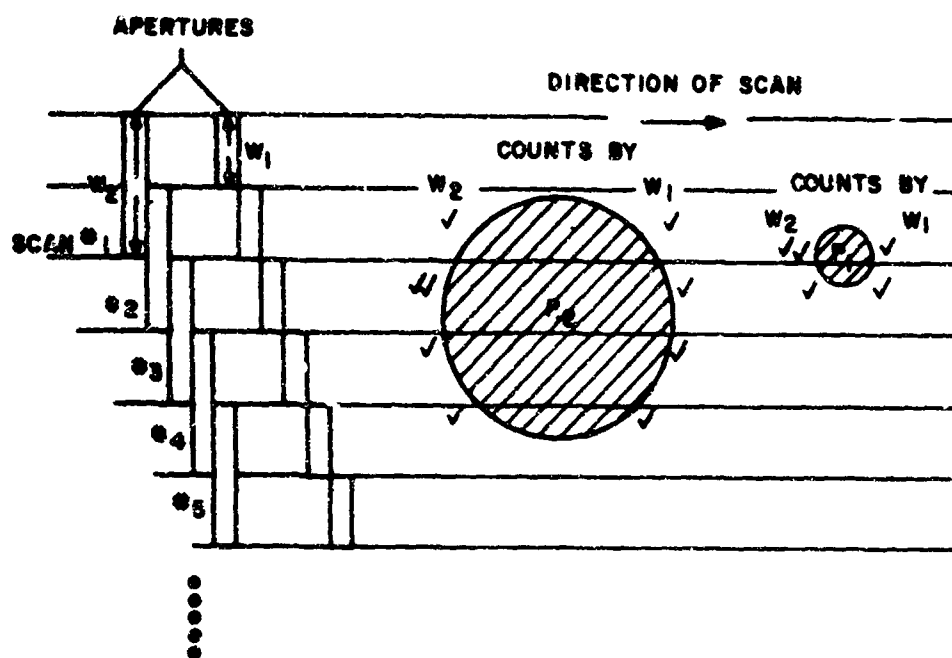


Fig. 3. Track-scanning geometry used in counting GAS aerosol data.

L = length of each scan,

W_1 = width of each scan, and

\bar{r} = average diameter of the particles.

If C equals the number of particles per unit area, then

$$N = \alpha L W_1 C. \quad (1)$$

The number of particles and fractions of particles ($p + f$) counted by the slit of width W_1 is

$$N_1 = \alpha C L (W_1 + \bar{r}), \quad (2)$$

and the slit of width W_2 is

$$N_2 = \alpha C L (W_2 + \bar{r}). \quad (3)$$

We can let $W_2 = 2 W_1$, and by eliminating \bar{r} between (2) and (3),

$$C = \frac{N_2 - N_1}{\alpha L W_1}. \quad (4)$$

But we know from Eq. (1) that

$$C = \frac{N}{\alpha L W_1};$$

therefore,

$$N = N_2 - N_1. \quad (5)$$

Accuracy of the Track-Scanning Method

1. Sources of Error. There are three types of error to be met when discussing the accuracy of particle counts. The first error results from trying to obtain information about the total particle population by just observing a sample of the particles. If the particles on the data area were arranged in an orderly fashion, a small sample would suffice to identify the population; however, in the case where the particles are randomly distributed, there is the question of whether we have chosen a sample truly representative of the population. This uncertainty is statistical in nature and can be expressed in terms of the Poisson distribution function. For a field of randomly distributed particles, the number of particles in sample areas is distributed according to the Poisson law, about their mean value with a variance equal to the mean. This indicates that the variance is also equal to the number of particles in the chosen sample area, since in a Poisson process the expected value equals the number counted.

For an indication of the relative accuracy of the count on a sample area, the coefficient of variation, which is the square root of the variance divided by the number counted, is used. From this we see that the statistical error can be reduced by choosing a larger sample size.

The second and third types of error are related to the scanning method. As mentioned before, the planar scanner was necessarily a compromise, since the instrument falls short of the capabilities of the human eye. The second error is thus caused by the inherent inability of the chosen scanning method to count accurately all the particles on the data area. However, this weakness of the scanning method can usually be described, and the effects of it predicted. The third source of error comes from the imperfect application of the scanning method to the data. Systematic and random errors of the scanner instrumentation are included in this category and will be described later.

2. Coincidence of Particles. The main cause of error in counting the GAS data with the track-scanning method is the coincidence of particles in the field of view of each slit. Since the particles are randomly distributed, it is possible to get two or more particles located close enough together so that the slit cannot resolve them. The result is a loss of counts and an incorrect number of particles on the data area.

LeBouffant et al (1954) and P. Hawksley (1954) have treated the coincidence problem for track scanning of circular particles which may be applied to our data as follows: Equation (6) was given by both authors as the basis for correction of the coincidence error.

$$\frac{N_i^*}{N_i} = \exp -n_i L_i, \quad (6)$$

where the subscript i refers to the particular slit in question, N_i is the number of $p + f$ which is actually on the data area, N_i^* is the lesser number of $p + f$ (because of coincidence) that the track-scanning method sees, n_i is the average number of $p + f$ per unit length of track scan, and L_i is the average length of the intercepts of the $p + f$. The length of each intercept is considered the distance on the data area along the direction of the scan in which the particle is visible in the scanning slit.

The use of Eq. (6) is valid only for paralyzable counters of type II as was noted by L. Takacs (1958) and W. Smith (1957). This type of counter remains inoperable for as long as it is exposed to individual or coinciding particles. Our counter was designed to approximate closely the above type; however, a long series of coinciding particles would cause several counts. There is a probability of having a long string of coinciding particles on our data area, in which case Eq. (6) would not be applicable; but this probability is small.

The number of $p + f$ per unit length of scan for our track-scanning method can be obtained from Eqs. (1), (2), and (3), and is given in Eqs. (7) and (8).

$$n_1 = \frac{N}{L} \left(1 + \frac{\bar{x}}{\bar{w}_1}\right), \quad (7)$$

$$n_2 = \frac{N}{L} \left(2 + \frac{\bar{x}}{\bar{w}_1}\right). \quad (8)$$

It should be noted that \bar{r} used in Eqs. (1) to (3) has been replaced by a different quantity \bar{x} . The reason for the change is that an electronic discriminator is necessary in the counting circuits to avoid spurious counts due to background noise. The effect on the average particle size is to reduce its vertical diameter by twice the distance that the slit must cover the particle to just obtain a countable pulse. This distance from the extreme edge of the particle to where the slit will first see the particle is z , and therefore,

$$\bar{x} = \bar{r} - 2z. \quad (9)$$

To obtain the mean length (L_1) of the intercepts of the $p + f$ on the data area, we have to divide the average total length of intercepts for each particle by the average number of times a particle is seen by the particular slit. For the slit of length W_1 , L_1 is given by Eq. (10).

$$L_1 = \frac{\bar{x} + \frac{\pi \bar{x}^2}{4 W_1}}{1 + \frac{\bar{x}}{W_1}} + W, \quad (10)$$

and for W_2 , L_2 is given by Eq. (11).

$$L_2 = \frac{2\bar{x} + \frac{\pi \bar{x}^2}{4 W_2}}{2 + \frac{\bar{x}}{W_1}} + W. \quad (11)$$

The numerator and denominator of the first term on the right in these equations consist of two parts. In the numerator the first part gives the length of the diameter of the particle, and the second part is the average total intercept length contributed by those portions of the particle which are seen by adjacent scans. Similarly, in the denominator, the first number is the count obtained from the diameter of the particle, while the second consists of the additional counts resulting from the portions of the particle extending into the adjacent scans. The slits both have a width W and this must be added to each mean intercept length. (It can be seen from the above two equations that an advantage of our track-scanning method is that the intercept that identifies each particle is from the widest part of each particle: the diameter.)

It should be mentioned that the \bar{x} in the numerator of Eqs. (10) and (11) is an approximation to the \bar{x} defined in Eq. (9). In finding the average total length of the intercepts for each particle, one presupposes the existence of circular particle of radius $\bar{x}/2$. This is not the case, since the existence of the discriminator effectively makes the circular images appear as an ellipse, with the longer dimension being larger than \bar{x} . If the value of z is small compared to the \bar{r} of the large particles, this source of error should be minor.

Combining Eqs. (6) through (11) and letting the width of each slit equal W_1 , we find that

$$\frac{N_1^*}{N_1} = \exp - \frac{N}{L} \left(2\bar{x} + \frac{\pi \bar{x}^2}{4 W_1} + W_1 \right), \quad (12)$$

and

$$\frac{N_2^*}{N_2} = \exp - \frac{N}{L} \left(3\bar{x} + \frac{\pi \bar{x}^2}{4W_1} + 2W_1 \right). \quad (13)$$

Realizing that \bar{x} can be expressed in terms of N and N_1 or N_2 , Eqs. (12) and (13) can be used to obtain the correction for the coincidence error experienced by the track-scanning method. We would need to solve only Eqs. (12) and (13) for N in terms of the machine counts of $p + f$, N_1^* , and N_2^* . Unfortunately, these equations are not implicit in N , so that the exact relationship desired cannot be derived. We can, however, construct a nomogram relating the machine count of $p + f$ to the value of N .

Noting that Eqs. (12) and (13) are implicit in N_1^* and N_2^* , respectively, and using Eqs. (2), (3), (5), and (9) to relate \bar{x} in terms of N and N_1 , we can solve for the machine count of $p + f$:

$$N_1^* = N_1 \exp - \frac{W_1}{L} (2N_1 - N + \frac{\pi}{4N} (N_1 - N)^2), \quad (14)$$

and

$$N_2^* = (N + N_1) \frac{N_1^*}{N_1} \exp - \frac{W_1 N_1}{L}. \quad (15)$$

To obtain coordinates for the nomogram curves, values of N and N_1 were chosen and Eqs. (14) and (15) solved for N_1^* and N_2^* . Since a large number of calculations were involved in constructing the nomogram of the desired range, an LGP-30 digital computer was used to solve the above equations. The calculations were chosen to cover all types of data one might expect to encounter from the GAS measurements. Below 100 particles on the data area, the coincidence error would be insignificant; hence, the nomogram was constructed with values of N ranging from 100 to 500. An additional necessary input was the average size of the particles on the GAS data. The range in average size \bar{x} was chosen from the smallest particle seen on the data areas to the largest.

Figures 4a through 4d show the computer results. The vertical and horizontal axes have the values of $p + f$ counted by the machine, and the solid lines are the values of the corresponding number of particles on the data area. To demonstrate the use of the nomogram, suppose that the scan of the data area with the slit of length W_2 gives an N_2^* count of 715 $p + f$ and the scan with the second slit an N_1^* count of 545 (see Fig. 4c). As can be seen, these coordinates correspond to 200 particles on the data area. If no correction for coincidence existed, and N_1^* and N_2^* were mistaken for N_1 , N_2 , then only 170 particles ($715 - 545$) would have been seen--a loss of 15 percent of the particles to coincidence.

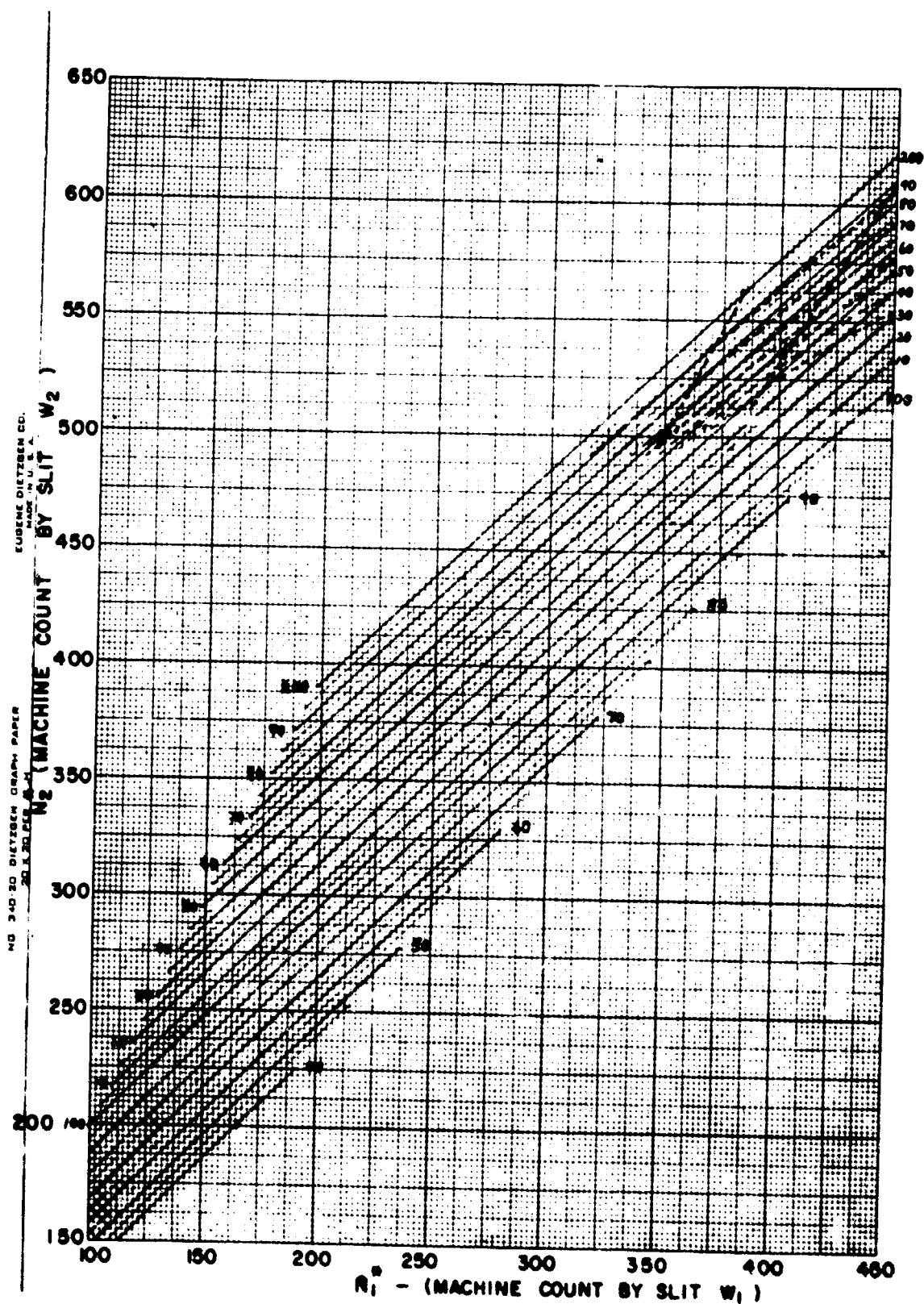


Fig. 4a

Figs. 4a-4d: Nomogram relating machine counts to actual number of particles on data areas. Dashed lines are the ϵ correction for the variable opacity of particle images.

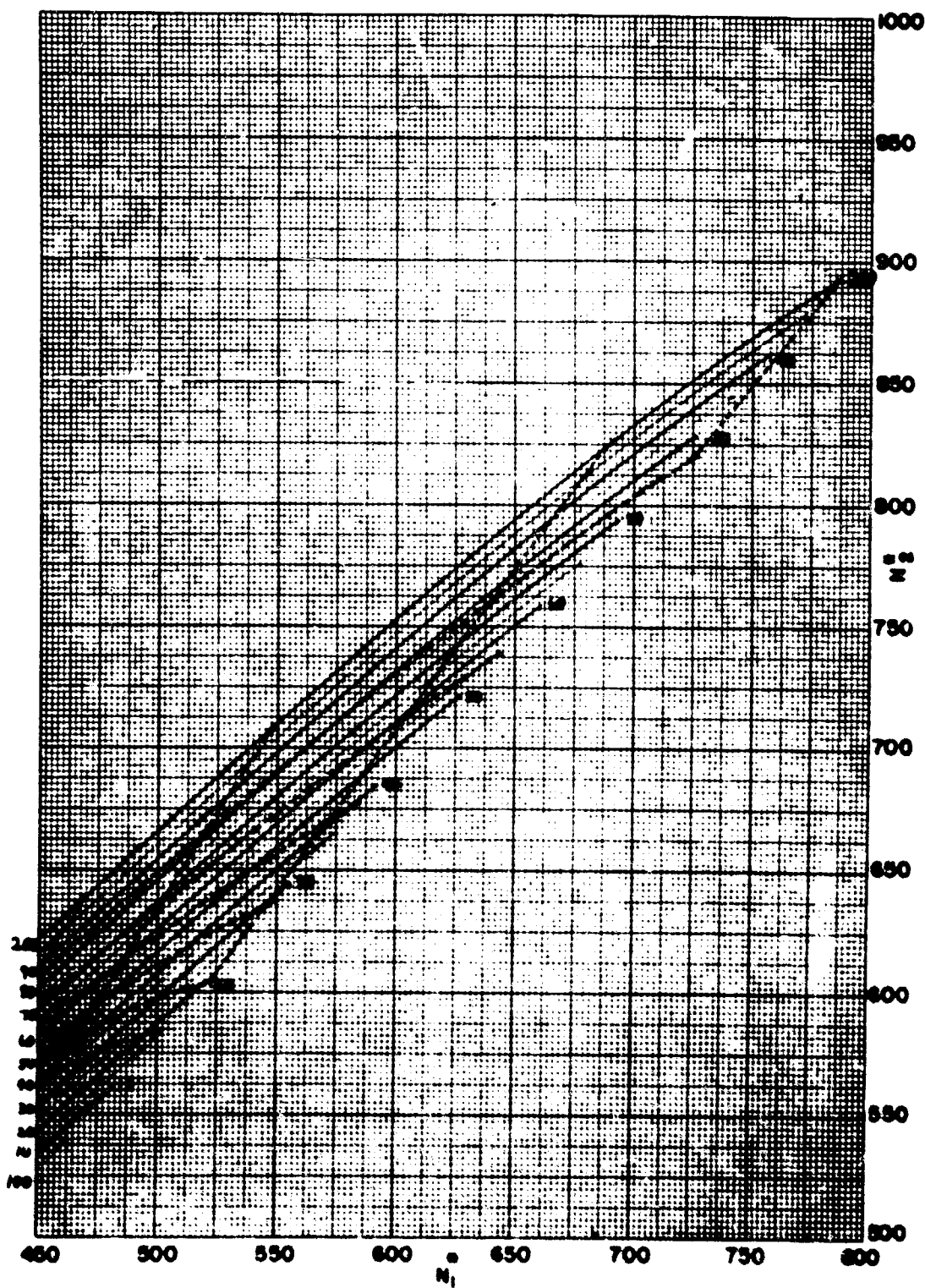


Fig. 4b

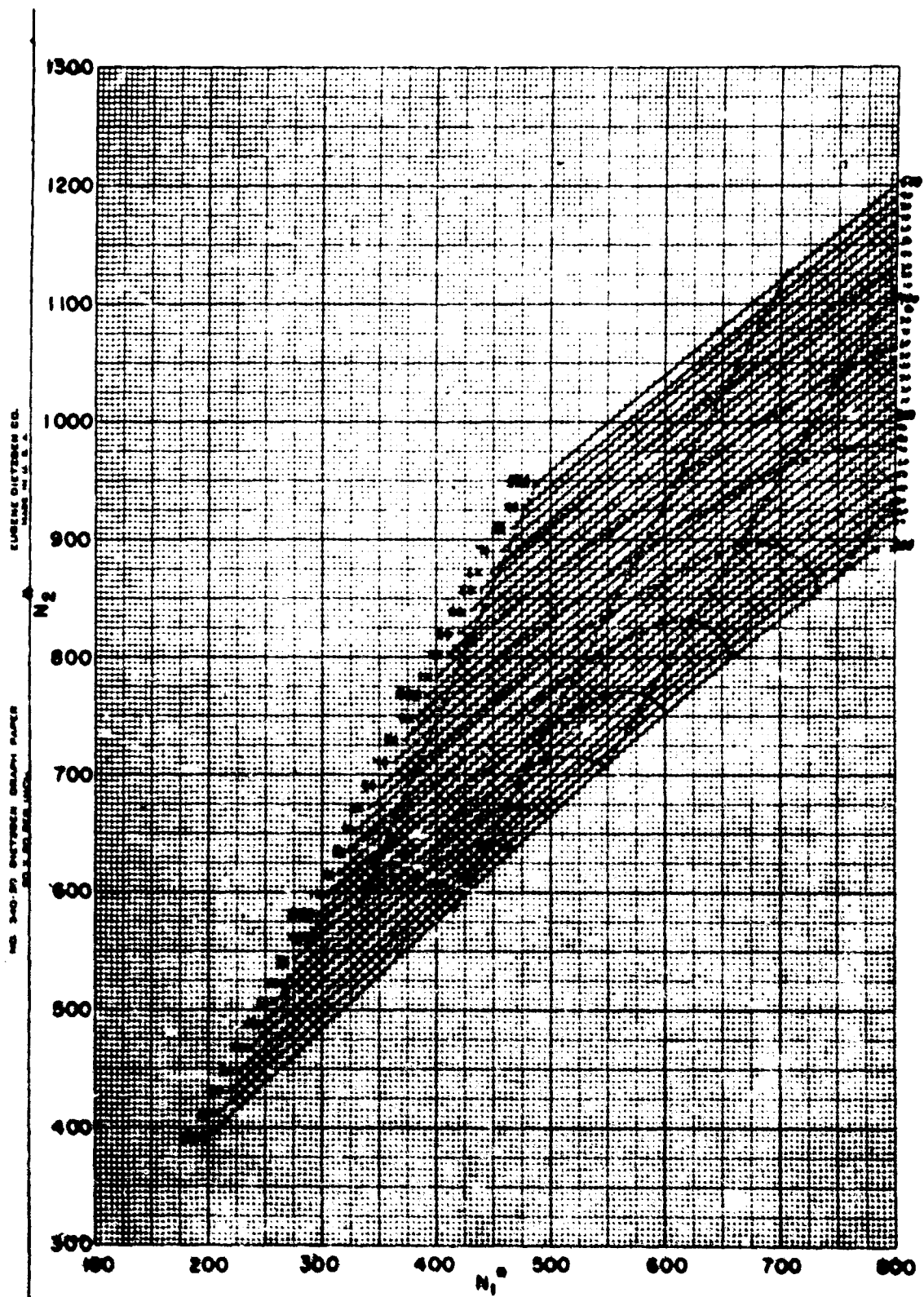


Fig. 4c

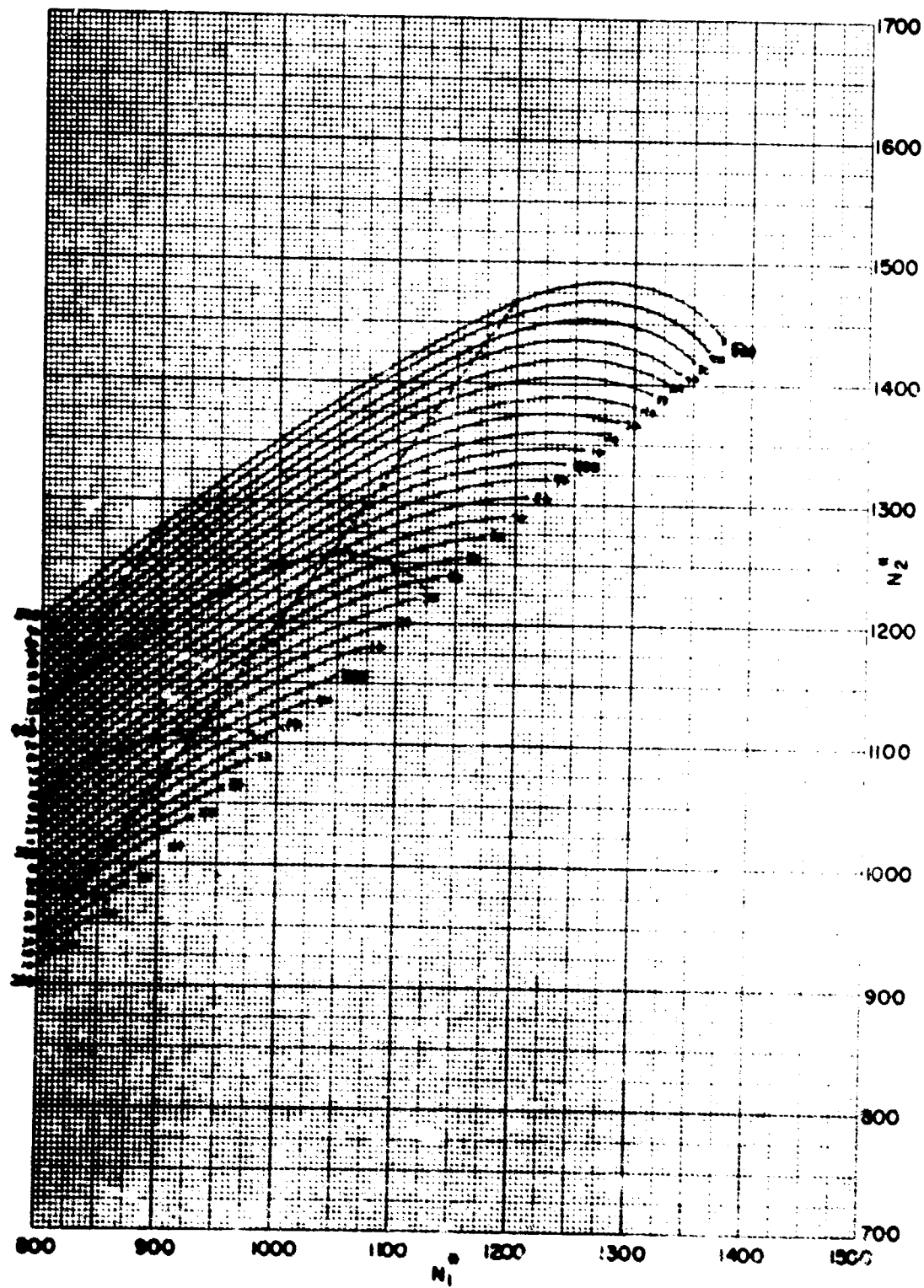


Fig. 4d

3. Variable Opacity of the Particle Image. The dashed lines on the nomogram are related to an additional correction which can be made for the coinciding particles. Remembering that Eqs. (12) and (13) were derived using \bar{x} as the size of the particles on the data area, it must be noted that this choice of the particle size is again an approximation to the actual size which should be used in Eqs. (12) and (13). A change from \bar{x} is necessary, since the $p + f$ which coincide act as if they are larger than the ones that are situated alone. This comes about because of the varying opacity of each particle and the existence of the electronic discriminator. These statements can be made clearer with the sketch in Fig. 5. Illustrated is the opacity cross-section of two particles as might be seen by the

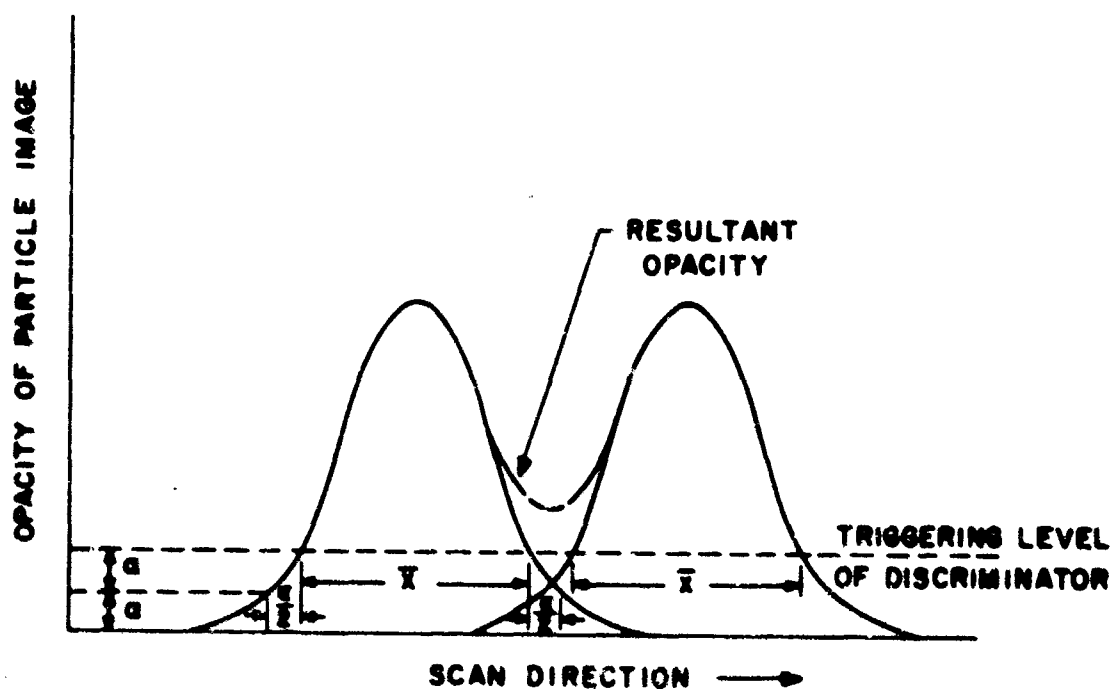


Fig. 5. Sketch of the opacity cross-section of two particles coinciding because of the addition of opacities in the tails of the particles.

phototube through either of the scanning slits. The particles are average in size and the intercepts are of the diameter of each.

From the figure it becomes evident that the addition of the opacity in the tails of the adjacent particles causes a loss of one count because of coincidence. Thus it is not correct to treat the coinciding particles as being of size \bar{x} , but of a slightly larger size $\bar{x} + \bar{\epsilon}$, where $\bar{\epsilon}/2$ is the average distance along the scan direction in which the opacity at the edge of the particle falls to just half of the value at the point where the opacity is equal to the discriminator level.

The error can be formulated as follows: Equations (2) and (3) are in the form of a linear relationship $N_i = h(W_i)$, which can be shown as a straight line (a) in Fig. 6. As can be seen, the slope of this line is N and the abscissa intercept is \bar{x} . It can be shown that a similar relationship, $N_i^* = k(W_i)$, exists for the $p + f$ counted by the machine and also for the $p + f$ considering the additional error, $N_{i\epsilon}^* = L(W_i)$. The former relationship is shown as line (b) and the latter as line (c).

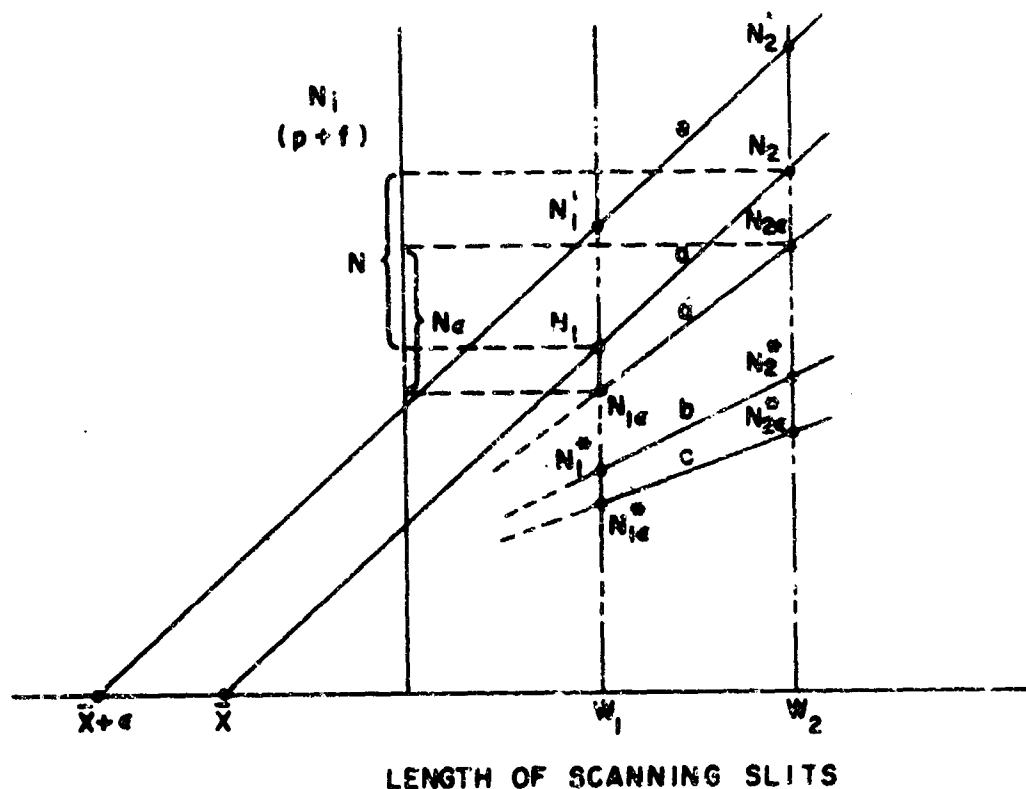


Fig. 6. Diagram used in the computation of the ϵ error.

In the actual machine count of $p + f$, the smaller quantities $N_{i\epsilon}^*$ are counted instead of N_i^* . When $N_{i\epsilon}^*$ is then used in Eq. (6) to find the correction due to coincidence, a quantity N_ϵ (line d) results, which is an underestimate of the true number of particles N . What is desired, therefore, is to obtain a relationship between N , N_ϵ , and the value of $\bar{\epsilon}$, for in this manner the constructed nomogram can be utilized.

From Fig. 6 we see that

$$N_\epsilon = N_{2\epsilon} - N_{1\epsilon}, \quad (16)$$

and using Eq. (5) in functional form, Eq. (16) becomes

$$N_{\epsilon} = N_{2\epsilon}^* \exp g(N_{\epsilon}, \bar{x}_{\epsilon}) - N_{1\epsilon} \exp f(N_{\epsilon}, \bar{x}_{\epsilon}) . \quad (17)$$

$$N_{1\epsilon} = N_1 - (N_1' - N_1^{*'}), \quad (18)$$

since the loss due to overlap of $p + f$ from the actual values of N_1 is given by the loss of $p + f$ from the particle population N' (see line c), whose average size is $\bar{x} + \bar{\epsilon}$, as shown in Fig. 6.

$N_1^{*'}$ is found from Eq. (6) to be

$$N_1^{*' } = N_1 \exp -f(N, \bar{x} + \bar{\epsilon}), \quad (19)$$

$$N_2^{*' } = N_2 \exp -g(N, \bar{x} + \bar{\epsilon}). \quad (20)$$

Also from Fig. 6 we see that

$$N_1' = N_1 + \frac{\bar{\epsilon}N}{W} . \quad (21)$$

On combining Eqs. (16) through (21), we find that

$$\begin{aligned} N_{\epsilon} = & \left\{ \left(N_2 + \frac{\bar{\epsilon}N}{W} \right) \exp -g(N, \bar{x} + \bar{\epsilon}) - \frac{\bar{\epsilon}N}{W} \right\} \\ & \exp g(N_{\epsilon}, \bar{x}_{\epsilon}) - \left\{ \left(N_1 + \frac{\bar{\epsilon}N}{W} \right) \exp -f(N, \bar{x} + \bar{\epsilon}) \right. \\ & \left. - \frac{\bar{\epsilon}N}{W} \right\} \exp f(N_{\epsilon}, \bar{x}_{\epsilon}); \end{aligned} \quad (22)$$

this is the desired result from which the effect of $\bar{\epsilon}$ on the coincidence correction can be obtained.

To use Eq. (22) to its fullest extent would mean the construction of a nomogram for each of various $\bar{\epsilon}$ values that might exist for different data areas. It would prove cumbersome to do this; therefore, an alternate procedure of plotting the ϵ correction on the constructed nomogram of Figs. 4a - d was tried.

As expected, Eq. (22) degenerates to Eqs. (12) and (13) when $\bar{\epsilon}$ is set equal to zero, so that the $p + f$ plotted in the nomogram would give us $N_{1\epsilon}$

when overlap is due only to particles of size \bar{x} . When the same group of particles is considered as being of size $\bar{x} + \bar{\epsilon}$, then $N_{1\epsilon}^*$ can be obtained from Eqs. (18), (19), and (20):

$$N_{1\epsilon}^* = N_1 - (N_1 + \frac{\bar{\epsilon}N}{W}) (1 - \exp -f(N, \bar{x} + \bar{\epsilon})), \quad (23)$$

$$N_{2\epsilon}^* = N_2 - (N_2 + \frac{\bar{\epsilon}N}{W}) (1 - \exp -g(N, \bar{x} + \bar{\epsilon})). \quad (24)$$

By combining Eqs. (23) and (24) with (12) and (13), we can write an expression for the change of the machine $p + f$ due to the use of a specific $\bar{\epsilon}$ value. This quantity will be called $\Delta N_{1\epsilon}^*$ (Eq. 25) and was plotted on the nomogram for various values of N and \bar{x} .

$$\Delta N_{1\epsilon}^* = N_{1\epsilon}^* - N_1^*. \quad (25)$$

The method used for plotting $\Delta N_{1\epsilon}^*$ was to choose an initial $p + f$ coordinate on the nomogram and apply Eq. (23). The $\bar{\epsilon}$ correction for that initial point was plotted on the nomogram and then was itself used for the next coordinate to be corrected with Eq. (25). This iterative procedure was done on various areas of the nomogram and resulted in the slanted dashed lines. The segments of the slanted lines, which are given by the intersection of the curved dashed lines, give the distance of $\Delta N_{1\epsilon}^*$ for the specific $\bar{\epsilon}$ that was used. This $\bar{\epsilon}$ was chosen to be equal to the average $\bar{\epsilon}$ value (γ) expected on the GAS data.

As noticed from the nomogram, the slanted lines are straight and the segments approximately equal for any small area of the nomogram. It thus becomes convenient to extrapolate the $\Delta N_{1\epsilon}^*$ value for areas that were not computed for this error. However, the question arises as to whether it would be possible to use the dashed lines to correct for an $\bar{\epsilon}$ value other than γ . The answer must be known, since the $\bar{\epsilon}$ for different GAS data could very likely vary around the value of γ . Preferably, a linear relationship should exist between the size of the $\bar{\epsilon}$ value and the distance along the lines of the γ correction. It does exist if the following two equations are valid:

$$\left. \sqrt{(\Delta N_{1\epsilon}^*)^2 + (\Delta N_{2\epsilon}^*)^2} \right|_{\gamma} = n \left. \sqrt{(\Delta N_{1\epsilon}^*)^2 + (\Delta N_{2\epsilon}^*)^2} \right|_{\epsilon_n}, \quad (26)$$

where $\epsilon_n = \frac{\gamma}{n}$, and $n = \frac{1}{5}$ to 5, and

$$\left. \frac{\Delta N_{2\epsilon}^*}{\Delta N_{1\epsilon}^*} \right|_{\gamma} = \left. \frac{\Delta N_{2\epsilon}^*}{\Delta N_{1\epsilon}^*} \right|_{\epsilon_n} \quad (27)$$

The Pythagorean theorem is used in Eq. (26) to show that multiples or fractions of γ result in proportional multiples or fractions of the plotted $\Delta N_{1\epsilon}^*$ value. The left part of Eq. (26) is evaluated with $\bar{\epsilon} = \gamma$, while the right part uses the multiple or fraction of γ , depending on the choice of n .

The second necessity for a linear relationship between the values of $\bar{\epsilon}$ and $\Delta N_{1\epsilon}^*$ is that the correction due to the multiple or fraction of γ lies in the same direction as the straight dashed lines. Equation (27) is used to show this, and it equates the slope of the γ correction with that of the multiple or fraction correction.

Equations (26) and (27) can be shown to be valid if the following approximations are made:

$$\exp - f(N, \bar{\epsilon}) = \exp - g(N, \bar{\epsilon}) \approx 1,$$

$$\frac{f(N, \bar{x} + \bar{\epsilon}_n)}{f(N, \bar{x} + \bar{\epsilon})} - \frac{g(N, \bar{x} + \bar{\epsilon}_n)}{g(N, \bar{x} + \bar{\epsilon})} \approx 0,$$

and

$$\exp - 2 f(N, \bar{x} + \bar{\epsilon}) \approx 1 + 2 \exp - f(N, \bar{x} + \bar{\epsilon}),$$

$$\exp - 2 g(N, \bar{x} + \bar{\epsilon}) \approx 1 + 2 \exp - g(N, \bar{x} + \bar{\epsilon}).$$

The error caused by these approximations is small compared to the value of the other terms in Eqs. (26) and (27), so that the change of $\Delta N_{1\epsilon}^*$ is approximately linear for various values of $\bar{\epsilon}$.

To demonstrate the correction for the ϵ error, let us refer to the nomogram coordinates used in the previous example. Suppose the measured ϵ were equal to $2/5 \gamma$. We would move from the $p + f$ coordinates of 715 and 545 to a new value of N along the straight dashed line. Since each segment of this line is equal to an $\bar{\epsilon}$ of γ , we would move $2/5$ of this distance to the correct value $N = 210$. In this example, coincidence error due to particles of size \bar{x} was 15 percent; and with the additional ϵ error, the total error increases to 20 percent.

4. Statistical Error. As was mentioned before, there is an unavoidable statistical error associated with the number of particles on a finite sample area. The amount of the error must be modified somewhat since

there are two contributors to the experimental count of the particles on that sample area. The final count is made up of the particles counted with the machine and the number that must be added because of the coincidence error. Both of these quantities have a statistical error associated with them, and according to L. LeBouffant et al (1954), the error can be expressed in terms of the Poisson law. The variance V of each quantity is equal to the value of each, and a total variance can be expressed as

$$\begin{aligned} V(\text{total}) &= V(\text{machine count} + \text{number of particles coinciding}) \\ &= V[N_{\epsilon}^* + (N - N_{\epsilon}^*)] \end{aligned} \quad (28)$$

Since the machine count and the particles that are coinciding are not independent of each other, Eq. (28) becomes

$$V(\text{total}) = V(N_{\epsilon}^*) + V(N - N_{\epsilon}^*) + 2\rho\sqrt{[V(N_{\epsilon}^*) V(N - N_{\epsilon}^*)]} \quad (29)$$

The correlation coefficient ρ is approximately equal to one, and substituting into Eq. (29) the values for the variances, the maximum total variance will be

$$V(\text{total}) = N + 2\sqrt{N_{\epsilon}^* (N - N_{\epsilon}^*)} \quad (30)$$

From Eq. (30) it is possible to find the range of the statistical error when using the machine to count the particles on the data area.

Description of Instrumentation

In the construction of the automatic counter, several requirements were stipulated. The most important of these was the necessity of scanning the data in a manner that would give the coverage described for the chosen track-scanning method. Especially important was the relationship of the scans of different widths with each other. If the relationship were not obtained, the claimed statistical accuracy would not result. The rapidity of evaluation of the data was the second concern in the building of the counter. It was decided that a rapid evaluation time would not be of prime importance if the entire counting process of a strip of 35-mm film data could be automated. This decision simplified the counter and made it possible to use mechanical instead of the faster but more complicated electronic scanning. A further simplification was the use of a precision projector to enlarge the film record of the data. In this manner the difficulty of scanning the film directly with accuracy measured in microns was eliminated.

The automatic counter, which was constructed at this Laboratory, is shown in Fig. 7. The approximate size of the instrument is 3 x 3 x 6 feet, and the panels which usually cover the sides of the instrument have been removed to show the interior components. To aid in the description of the counter, a flow diagram is illustrated in Fig. 8.

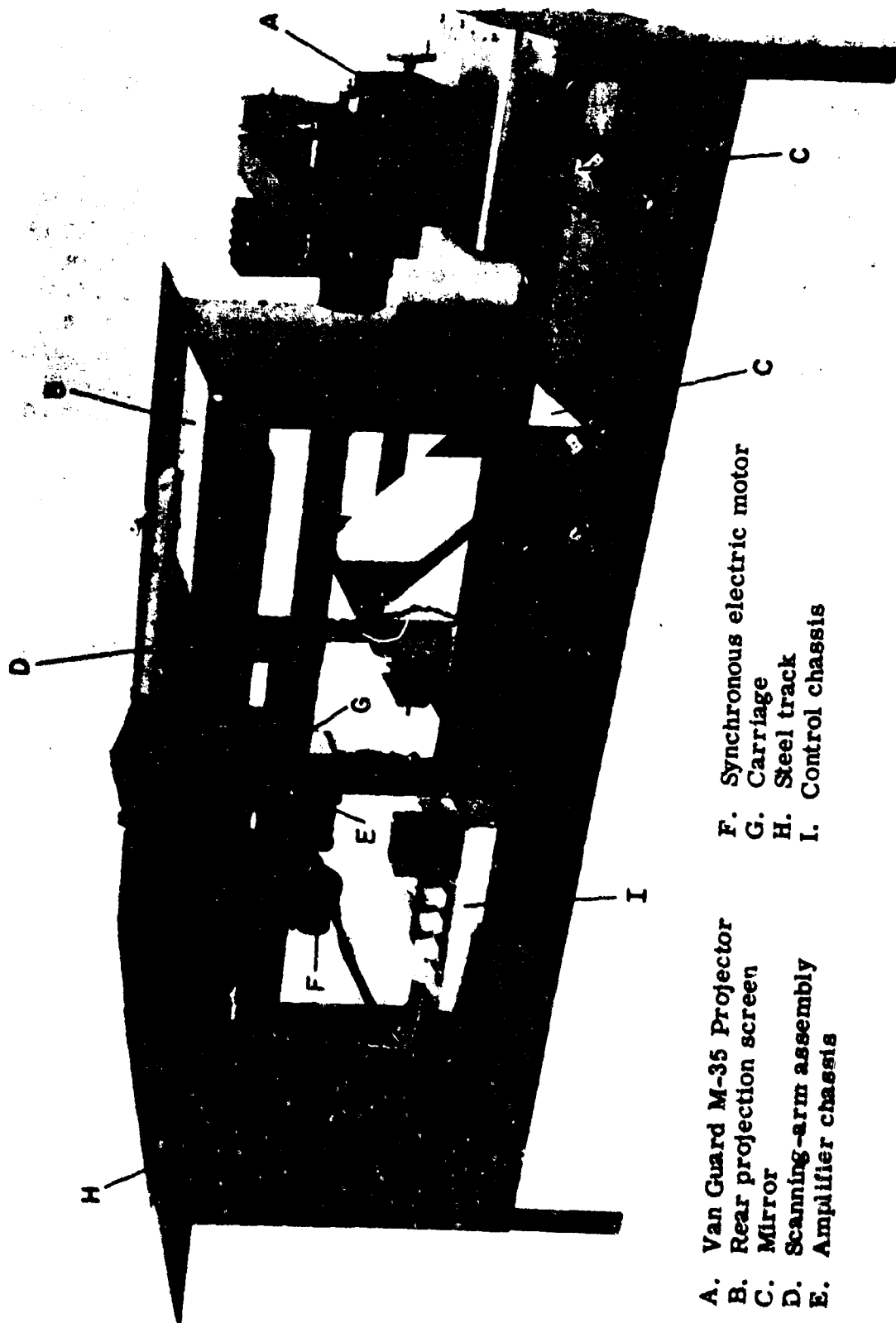
1. Optics. A Van Guard M-35 projector (A), which has the capabilities of automatically advancing the film strip and of positioning each frame with a fraction of one mil accuracy, is used to project the information on a rear projection screen (B). The diagonally-mounted mirrors (C) are used to direct the downward projected light to the undersurface of the screen. The magnification from the film to the screen is about 50, so that the particle images on the film are increased to a size on the screen of between 1/16 and 1/4 inch in diameter. The scanning-arm assembly (D) is located directly over the top of the screen, which can transmit diffuse light. Essentially, the assembly consists of a hollow tube that channels the light flux from a specific area on the screen to the photomultiplier. This is accomplished as follows: A small diagonal mirror, located at the end of the arm, directs the light from the screen into the tube. The light passes through several achromat lenses and a field stop in the form of a slit. The dimensions of the slit, which are equivalent to the size of the area being inspected on the screen, can be continuously adjusted with a micrometer for both length and width.

For the GAS data, the slit length was chosen to be 1/16 inch for W_1 , and 1/8 inch for W_2 . It was felt that these dimensions were a good compromise, since a larger size would increase the coincidence losses and a smaller size would decrease the signal-to-noise ratio.

After passing through the field stop and the horizontal portion of the scanning arm, the light makes another 90-degree change in direction and falls on the photomultiplier situated in the amplifier chassis (E).

2. Mechanics. The chassis, scanning-arm assembly, and also a synchronous electric motor (F), are mounted on a carriage (G). The motor has the dual function of sliding the carriage along steel tracks (H) and of rotating the scanning arm about a vertical axis and in the plane of the screen. Both motions are coupled so that the tip of the rotating scanning arm describes a closely reproducible helical path over the top surface of the counter. By synchronizing the rate of rotation of the arm with the movement of the carriage along the tracks, the entire screen can be scanned with consecutive passes of the arm which are separated by the desired length of the smaller slit. The rate of rotation of the arm is 2 rps so that the 140 passes which cover the entire screen take a little over one minute in time.

3. Electronics. The light fluctuations received at the amplifier from the scanning arm passing over the screen must next be changed into



A. Van Guard M-35 Projector
 B. Rear projection screen
 C. Mirror
 D. Scanning-arm assembly
 E. Amplifier chassis

F. Synchronous electric motor
 G. Carriage
 H. Steel track
 I. Control chassis

Fig. 7. Automatic particle counter

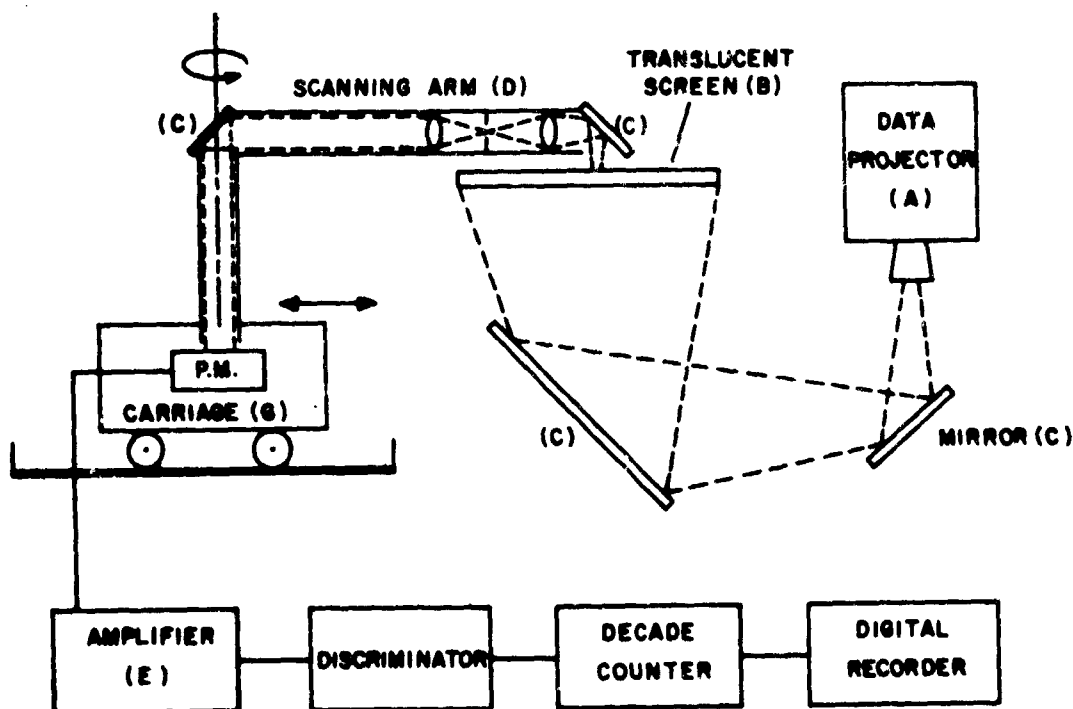


Fig. 8. Principal components of the automatic counter

electrical signals so that they can be counted. In considering the design of the amplifier, we should remember the need for a paralyzable counter of type II. For this reason the output signals of the amplifier were designed to reproduce closely the waveforms of the pulses of light received at the photomultiplier. For instance, if the amplifier produced only an electronic pulse from the front edge of the particles or integrated the fluctuation from the particle, the counter would not remain inoperable for the duration of slit passage over the particle, and the coincidence equations and nomogram would not be valid.

A direct consequence of the necessity of the amplifier in providing an output without distortion is the choice of the width of the scanning slit. If the slit were narrow, the variations in the particle opacity due to the diffraction pattern would be reproduced by the amplifier, and more than one count might be obtained by each particle. To prevent the additional counts, the width of the scanning slits was chosen to be larger than the separation of the concentric circles in the diffraction pattern. For the GAS data, the width amounted to 1/16 inch for both slits.

The electronics of the amplifier consist of a ten-dynode type photomultiplier followed by a clamping circuit, two stages of negative feedback

stabilized amplification, and a cathode follower. The desired function of the photomultiplier is to change the light fluctuations into electrical signals in a manner which is similar for each slit used. Since the background light flux from the screen is twice as much for the larger slit than for the smaller one, the coordinates of the d.c. point on the load line for the photomultiplier are different for each slit. It is possible, therefore, to obtain signals from the same particle which are different in amplitude for each slit. This difference can be tolerated for the denser center portions of the particle, but for the area of the particle which is of the opacity necessary to trigger the discriminator, the difference would make the track-scanning method inoperable. By choosing to operate the photomultiplier in a portion of the anode dynamic characteristic, where small fluctuations from the quiescent point corresponding to each slit are equivalent for the same fluctuations in the light intensity, the discriminator would see the particle as being the same size for each slit.

The clamping circuit, which consists essentially of a diode in parallel with the photomultiplier, is needed to eliminate the large square wave formed by the background light level on the screen. The circuit in effect raises the pulses formed by the particles and situated on the negative portion of the square wave to a zero potential reference. In this manner a change in the light intensity used to project the data would not necessitate a change in the discriminator level. Also, a pulse, useful for the calibration of the light source and photomultiplier, is formed by the following edge of the screen.

To avoid distortion of the electric pulses produced by the light fluctuations, the amplifier was constructed to act as a passive band pass filter which had a frequency response wide enough to cover the frequencies presented by the passage of the slits over the particles. The required frequency range was 1 to 10 kc. By a correct choice of the capacitance values in the coupling between stages, the low frequency distortion caused by the 120 cps component of the tungsten projection bulb was reduced to an acceptable value without excessive attenuation above 1 kc. For the upper half-power frequency, a shunt capacitor was used, and the high-frequency noise from the photomultiplier and triode vacuum tubes was reduced.

The output of the amplifier is fed directly to the discriminator, which consists of a Schmidt trigger circuit. The operation of this circuit is to produce a pulse whenever a preset level in the input signal is reached. For the input signals produced by the particle images, the circuit triggers from the leading edge of each signal and remains inoperable for the duration of the passage of the slit over that particle. The pulses from the Schmidt circuit are recorded on the tape readout of a Hewlett-Packard digital recorder. (Both the discriminator and decade counters are modified components of an existing instrument, a Royco PC-200A particle counter, and along with the digital recorder, are not shown.)

The last item on Fig. 7 to be discussed is the control chassis (I), with which it is possible to automate the evaluation of a long film strip. The functions of (I) are as follows: When the scanning arm has reached either extremity of the screen, a microswitch located on the steel track is tripped by the carriage, and one of the five relays on the chassis is activated. This initiates a sequence in which the number of counts on the decade counter is printed out by the digital recorder, the synchronous motor is stopped, the Van Guard projector advances the film strip one frame, the decade bank is reset to zero, and the motor is again started, but in the reverse direction. The entire process takes approximately two seconds and is repeated for each frame of the film. After the film strip has been scanned, it must be manually reloaded onto the projector to be scanned again with the second slit.

Evaluation of the Automatic Counter

In this section we analyze the capabilities of the automatic counter to count particles accurately. The questions which we will try to answer are: Is the choice of the scanning method valid for the particle data? is the application of the scanning method exact? or do counting errors exist because of errors in the optics, mechanics, or electronics of the instrumentation? and is it possible to rely on the predicted statistical error of the machine counts?

These questions can be answered by operating the instrument with known data and comparing the results. For a reliable estimate of the accuracy of the instrument, many comparisons should be made and the known data should have a range similar to that which the instrument will encounter in practice. And, of course, the data used as the standard should be very accurately documented. Such a rigorous evaluation of the counter was not performed; instead, only a few comparisons were made with samples of visually evaluated GAS data. Considering the fact that particle data might exist with different characteristics than those of the samples, and remembering that visual evaluation is not the most reliable method, the accuracy claims in this section will probably need further substantiation.

The first comparison of the number of particles counted with the instrument and those by visual examination of the GAS data was obtained during the process of choosing the correct high-voltage value for the operation of the photomultiplier. A frame of a GAS data film was chosen and counted several times with the automatic counter and its nomogram corrections. For each count, another high-voltage value (at constant discriminator level) was used for the photomultiplier. After also counting the frame visually, the counts versus high voltage were plotted (Fig. 9).

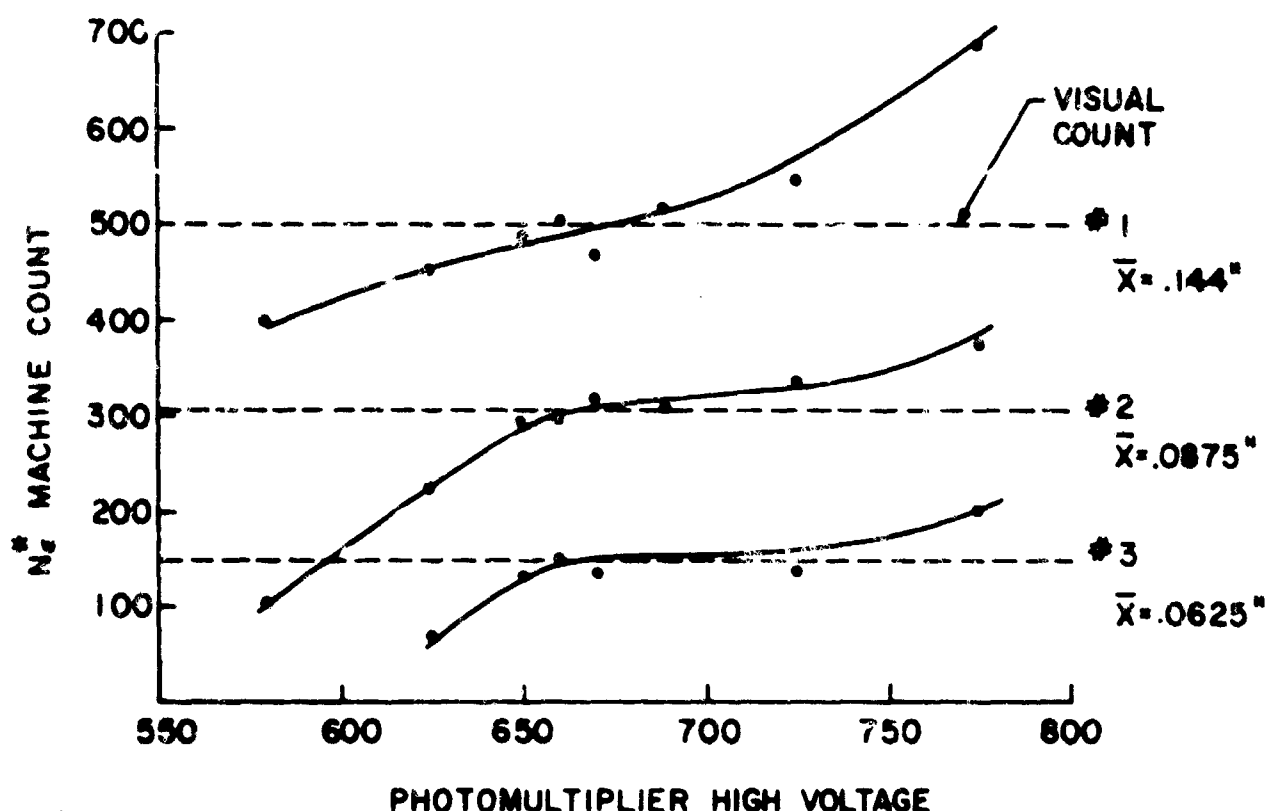


Fig. 9. Machine counts of three frames of GAS data film

The obvious choice of the high voltage to be used for operation is at the point in Fig. 9 where the instrument's curve (No. 1) intersects the visual value. To confirm this choice, two other frames of film data were evaluated in the same way (see curves No. 2 and No. 3). For all three frames the correct operating high voltage was found to be approximately 670 volts.

For added significance of this first comparison, the three frames were chosen so that the average size, \bar{x} , of the particle images was different for each (see Fig. 9). The fact that the machine counts with the same sensitivity of the photomultiplier agree with the visual count for all three frames shows that the instrument can count independently of size and that no large systematic errors exist in the application of the scanning method nor in the instrumentation.

To determine whether smaller random errors exist in the machine counts that would not have been seen in the first comparison, a second comparison was made, using the chosen high voltage. One frame of the GAS data was picked and was evaluated repeatedly with the automatic counter. If no additional random errors existed, the many machine counts of the one frame would all be of the same value. The following weaknesses in the instrumentation could, however, furnish reasons for variations in the number counted: Inaccurate positioning of the film by the

projector for the scan with each slit; the scanning arm does not scan the screen as precisely as given in Fig. 3; or the noise in the electronics has not been eliminated to a sufficient degree to prevent spurious signals.

Figure 10 shows the results of this test, and, as can be seen, some variations do exist in the count. It was assumed that the size of the

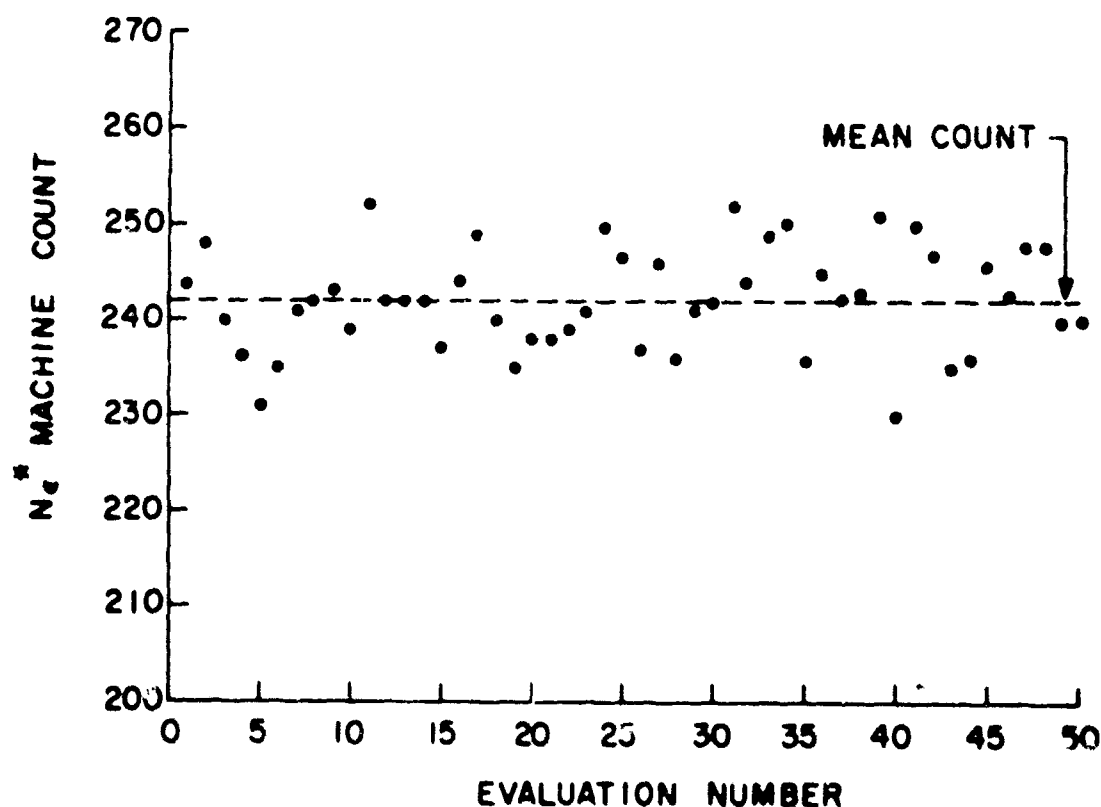


Fig. 10. Repetitive machine count of one frame of GAS data film

fluctuations was normally distributed about the mean count and a variance S^2 was computed. The value of S^2 was found to be 29.8. This small value is a good indication that none of the above weaknesses exist to any great extent, since for scans of two slits, which take independent paths over the same data area, the variance could be as high as the mean of the total number counted by both slits (P. Hawkey, 1954). Also, if we compute the variance of the total statistical error for this sample as if it were part of an actual test ($V = 312$; Eq. (30)), we see that the above-described random error is almost insignificant. If it is desired to include this small error, its standard deviation can be added geometrically to the standard deviation given by Eq. (30).

The last comparison is a machine and visual evaluation of an actual GAS field test conducted in the Flagstaff, Arizona, area during the summer of 1965. The evaluation was made since it gave the counter the opportunity of showing its applicability to a wider range of data than was found in the prior comparisons. It also provided the opportunity to test the validity

of the expected statistical error given in Eq. (30), a test that would show the overall accuracy of the counter.

Fifty-six microphotographs were taken of the 30 July test, and the resulting particle counts are shown in Fig. 11 where the number of

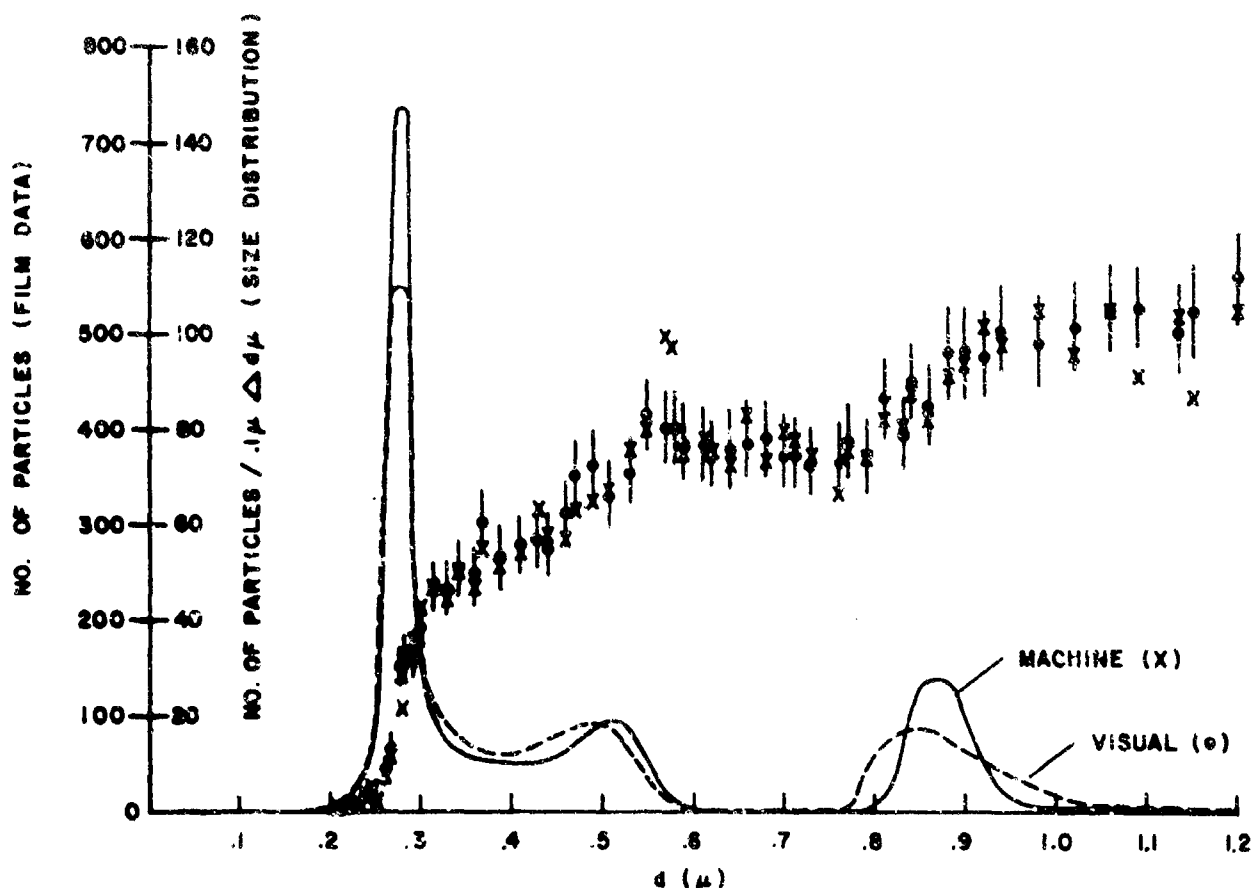


Fig. 11. GAS field test, 30 July 1965, Flagstaff Arizona. Short vertical lines are the predicted 95 percent confidence intervals for the machine counts. Smooth curves give the size distribution obtained by differentiating mean curves (not shown) drawn through the visual and machine points.

particles on each frame is plotted as a function of their Stokes diameter. One can see that the machine and visual counts compare favorably for most of the frames over the entire range of data; however, some fluctuations do exist between the two counts. The differences were to be expected, since the statistical error of the "true" visual count is due only to the sample size; while for the machine count the additional uncertainty exists because of particles coinciding and the small random instrument error mentioned

previously. The variance of these fluctuations should be equivalent to the value given by the second term of Eq. (30) and can be used in this manner to test the operation of the counter. If the fluctuations of the instrument count are much larger than that permitted by the second term of Eq. (30), then the instrument is not operating properly. However, if the fluctuations are within a certain interval of computed uncertainty, then the reverse is true.

The method of confidence intervals can be used to determine which of the above criteria can be accepted. First, the variance for the coincidence of the particles is computed for each of the visually evaluated counts. Also, we know that this group of particles is distributed about their mean according to the Poisson law for small numbers, and Normal law for large numbers. We can therefore use tables to find the confidence interval for each of the visually evaluated points.

A confidence interval of 95 percent was chosen and is drawn as a small vertical line for each of the visual points in Fig. 11. The distance that each line covers corresponds to a 95 percent certainty of finding the experimental value in that location. In other words, if approximately 95 percent of the machine counts fall within this interval, the counter can be considered to be operating correctly.

As can be seen from Fig. 11, fifty of the fifty-six measured values fall into the confidence intervals. The ratio of machine counts falling into the intervals is thus only 0.89 instead of the predicted ratio of 0.95. This difference could be due to chance, since the counts are random samples. Using the binomial law and the measured 0.89 ratio, we can say that there are eight chances out of ten that the true ratio of the machine count will be between 0.79 and 0.96. The predicted ratio of 0.95 is included in this interval just so that, with the above-mentioned chance, the desired criterion can be accepted.

Strictly speaking, these favorable results are applicable only to the test of 30 July. However, since many of the other data collected with the GAS are similar to those of 30 July, the counter can probably be applied to those data also.

ACKNOWLEDGMENTS

Special credit and thanks are due to Messrs. Frank Trussel and Henry Riesbsamen, Engineering Support Services Dept, USAECOM, for their excellent design and construction work on the automatic counter. Appreciation is expressed to the following personnel of Atmospheric Sciences Laboratory: Dr. Helmut Weichmann* for his efforts in initiating this scientific

*now with the Department of Commerce

effort and to Mr. Marvin Lowenthal for his continued support and encouragement. Appreciation is extended to Messrs. Raymond Belucci and Anthony Barichivich for assistance in the preparation of the computer program; to Dr. Richard Schottland for constructive criticism of the text of the report; to Mr. Andrew Petriw for his aid in rewriting a portion of the text; and to Mrs. Christiana Jorgensen for her dedicated and professional editing and preparation of the report.

REFERENCES

- Adler, C. R.; Mark, A. M.; Marshall, W. R., Jr.; and Parent, R. J., 1954: A Scanning Device for Determining the Size Distribution of Spray Droplet Images. Chemical Engineering Progress, 50, No. 1, pp 14-23.
- Biggs, R.; MacMillan, R. L., 1948: Counting Techniques of Red Blood Cells. J. of Clinical Pathology, 1, p 269.
- Casella (Electronics), Ltd., Automatic Particle Counter and Sizer, 46/48, Osnaburgh St., London N. W. 1, England.
- Cinema-Television, Ltd., Flying-Spot Particle Resolver. Worsley Bridge Road, Lower Sydenham, London, S. E. 26, England.
- Connor, P., 1963: Automatic Counting and Sizing of Particles. Industrial Chemist, 39, No. 2, pp 69-74.
- Cooke-Yarborough, E. H.; and Whyard, R. E., 1954: The Automatic Counting of Red Blood Cells. British J. of Applied Physics, Supplement 3, pp S147-S165.
- Courshee, R. J., 1954: Testing A Counting Machine. ibid, Supplement 3, pp S161-S165.
- Dell, H. A.; and Jones, E., 1951: British Patent 741, 471.
- Dell, H. A.; Hobbs, D. C.; and Richards, M. S., 1960: An Automatic Particle Counter and Sizer. Phillips Technical Review, 21, pp 253-280.
- Flory, L. E; and Pike, W. S., 1953: Particle Counting by TV Techniques. RCA Review, 14, pp 546-556.
- Gillings, D. W., 1950: British Patent Application 11078/50.
- Goetz, A.; Stevenson, H. J. R.; and Preining, O., 1960a. The Design and Performance of the Aerosol Spectrometer. J. of the Air Pollution Control Association, 10, No. 5, pp 378-383, 414, 416.

Goetz, A.; Preining, O., 1960b: The Aerosol Spectrometer and Its Application To Nuclear Condensation Studies. Physics of Precipitation, American Geophysical Union Publication No. 746.

Hawksley, P. W., 1954a: Theory of Particle Sizing and Counting By Track Scanning. British J. of Applied Physics, Supplement 3, pp S125-S132.

Hawksley, P. W.; Blackett, J. H.; Meyer, E. W.; and Fitzsimmons, A. E., 1954b: The Design and Construction of A Photoelectric Scanning Machine for Sizing Microscopic Particles. ibid., Supplement 3, pp S165-S147.

LeBouffant, L.; and Soule, J. L., 1954: The Automatic Size Analysis of Dust Deposits By Means of An Illuminated Slit. ibid., Supplement 3, pp S143-S147.

Morgan, B. B.; and Meyer, E. W., 1959: Multichannel Photoelectric Scanning Instrument for Sizing Microscopic Particles. J. of Scientific Instruments, 36, pp 492-501.

Mullard, Ltd., Film Scanning Particle Analyzer. Equipment Division, Mullard House, Torrington Place, London, W. C. 1, England.

Pearson, J. E.; and Martin, G. E., 1957: Automatic Sizing and Counting of Stains or Images, pp 99-107, in An Evaluation of Raindrop Sizing and Counting Techniques, in cooperation with Dept. of General Engineering, U. of Illinois, Scientific Report No. 1 under Contract No. AF 19 (604) - 1900.

Phillips, J. W., 1954: Some Fundamental Aspects of Particle Counting and Sizing By Line Scans. British J. of Applied Physics, Supplement 3, pp S135-S136.

Smith, W. L., 1957: On Renewal Theory, Counter Problems, and Quasi-Poisson Processes. Proceedings of the Cambridge Phil. Society, 53, pp 175-177.

Takacs, L., 1958: On A Probability Problem In The Theory of Counters. Annals of Mathematical Statistics, 29, pp 1257-1259.

Walton, W. H., 1954: Survey of The Automatic Counting and Sizing of Particles. British J. of Applied Physics, Supplement 3, pp S121-S125.

Wheeler, L. K.; and Trickett, E. S., 1953: Measurement of The Size Distribution of Spray Particles. Electronic Engineering, 25, pp 402-406.

Unclassified

Security Classification		
DOCUMENT CONTROL DATA - R & D		
(Security classification of title, body of abstract and indexing annotation must be entered when the overall report is classified)		
1. ORIGINATING ACTIVITY (Corporate author) U. S. Army Electronics Command Fort Monmouth, N. J. 07703		2a. REPORT SECURITY CLASSIFICATION Unclassified
		2b. GROUP
3. REPORT TITLE AUTOMATIC COUNTING OF ATMOSPHERIC AEROSOLS COLLECTED WITH THE GOETZ ULTRACENTRIFUGE		
4. DESCRIPTIVE NOTES (Type of report and inclusive dates) Technical Report		
5. AUTHOR(S) (First name, middle initial, last name) Hermann E. Gerber		
6. REPORT DATE June 1967	7a. TOTAL NO. OF PAGES 33	7b. NO. OF PAGES 24
8a. CONTRACT OR GRANT NO.		8b. ORIGINATOR'S REPORT NUMBER(S) ECON-2852
a. PROJECT NO. IV0-14501-B-53A		
c. Task No. -03		9b. OTHER REPORT NO(S) (Any other numbers that may be assigned this report)
d.		
10. DISTRIBUTION STATEMENT Distribution of this document is unlimited.		
11. SUPPLEMENTARY NOTES Development of automatic counter for evaluation of aerosol data collected with GAS ultracentrifuge.		12. SPONSORING MILITARY ACTIVITY U. S. Army Electronics Command ATTN: AMSEL-BL-AP Fort Monmouth, N. J. 07703
13. ABSTRACT An automatic counter was developed with which submicron aerosol data, collected with the Goetz Aerosol Spectrometer ultracentrifuge was rapidly and accurately evaluated. The data, consisting of 35mm microphotographs of large numbers of aerosols, were reduced by utilizing a unique track-scanning geometry in conjunction with a mechanical planar scanner. The photographic images of the aerosols and their locations on the data field were considered in detail, and appropriate corrections were derived to compensate for coincidence counting losses and the variable opacity of the images. Using the automatic counter, it was possible to count up to 500 aerosol images on a 2.0 cm ² area on each microphotograph. The counts were accomplished with a standard deviation of approximately 0.20 times the magnitude of the inherent statistical uncertainty of the data; also, each microphotograph was automatically scanned and counted in 140 seconds.		

DD FORM 1473

REPLACES DD FORM 1473, 1 JAN 64, WHICH IS
OBSOLETE FOR ARMY USE.

(1)

Unclassified

Security Classification

